HHS Public Access

Author manuscript

Metabolism. Author manuscript; available in PMC 2019 August 01.

Published in final edited form as:

Metabolism. 2018 August ; 85: 76–89. doi:10.1016/j.metabol.2018.03.002.

Depletion of dendritic cells in perivascular adipose tissue improves arterial relaxation responses in type 2 diabetic mice

Tianyi Qiu[1,2], **Min Li**[1], **Miles A. Tanner**[1], **Yan Yang**[1], **James R. Sowers**[1,2], **Ronald J. Korthuis**[1,2], and **Michael A. Hill**[1,2]

[1]Dalton Cardiovascular Research Center, University of Missouri and Truman VA Medical Center, Columbia, Missouri 65211, USA

[2]Department of Medical Pharmacology and Physiology, University of Missouri and Truman VA Medical Center, Columbia, Missouri 65211, USA

Abstract

Background—Accumulation of multiple subtypes of immune cells in perivascular adipose tissue (PVAT) has been proposed to cause vascular inflammation and dysfunction in type 2 diabetes (T2DM). This study was designed to investigate specific roles for dendritic cells in PVAT in the development of vascular inflammation and impaired PVAT-mediated vasorelaxation in T2DM.

Methods and Results—Studies were performed using *db/db* mice (model of T2DM) and their Db heterozygote (DbHET), lean and normoglycemic controls. Dendritic cell depletion was performed by cross-breeding DbHet with Flt3l$^{-/-}$ (null for ligand for FMS-kinase tyrosine kinase) mice. Using PCR, it was found that the majority of dendritic cells (CD11c^{+}) were located in PVAT rather than the vascular wall. Flow cytometry similarly showed greater dendritic cell accumulation in adipose tissue from *db/db* mice than DbHET controls. Adipose tissue from *db/db* mice displayed increased mRNA levels of proinflammatory cytokines TNF-α and IL-6 and decreased mRNA levels of the anti-inflammatory mediator adiponectin, compared to DbHET mice. Depletion of dendritic cells in db^{Flt3l-}/db^{Flt3l-} (confirmed by flow cytometry) reduced TNF-α and IL-6 mRNA levels in diabetic adipose tissue without influencing adiponection expression. Moreover, in mesenteric arteries, dendritic cell depletion improved the ability of PVAT to augment acetylcholine-induced vasorelaxation and anti-contractile activity.

Corresponding author: Michael A. Hill, Ph.D. Professor of Physiology, Dalton Cardiovascular Research Center, University of Missouri, 134 Research Park Drive, Columbia, MO 6521, hillmi@missouri.edu, Telephone: 573-882-9662.

Author Contributions

TQ was responsible for performance of experiments, data presentation and writing of the manuscript. ML, MAT and YY were responsible for performing specific experiments and editing of the manuscript. RJK and JRS contributed to experimental design, data interpretation and editing of the manuscript. MAH contributed to study design, data interpretation, writing and editing of the manuscript.

Disclosures

None.

Conclusions—In a murine model of T2DM, dendritic cells accumulated predominantly in PVAT, as opposed to the vessel wall, per se. Accumulation of dendritic cells in PVAT was associated with overproduction of pro-inflammatory cytokines, which contributed to an impaired ability of PVAT to augment vasorelaxation and exert anti-contractile activity in T2DM.

Keywords

immune cells; chronic inflammation; vasodilation; anti-contractile function; cytokines

1. Introduction

The prevalence of obesity, type 2 diabetes (T2DM) and associated cardiovascular disease (CVD) are rising, globally [1]. Obesity, especially central obesity, is believed to contribute to the progression of T2DM and associated CVD [2]. As a result, the role of specific fat stores in promoting CVD in these populations is an area of active investigation.

Adipose tissue has traditionally been considered as an energy storage depot [3]. However, more recent studies have indicated that adipose tissue is an active immunological organ, harboring various immunocytes and a number of bioactive and inflammatory molecules [4]. Indeed, inflammatory immune cells, such as macrophages [5], B[6] and T lymphocytes[7] accumulate in adipose tissues in obese murine models. Importantly, in obesity these adipose tissue immune cells appear to cause excess secretion of pro-inflammatory cytokines, including tumor necrosis factor alpha (TNF-α), interleukin 6 (IL-6) and interferon-gamma (IFN-γ). The pro-inflammatory environment promotes infiltration of additional adipose tissue immune cells creating a vicious circle. This situation further enhances the inflammatory response, promoting insulin resistance, the development of T2DM and associated CVD [4, 8, 9].

Perivascular adipose tissue (PVAT), defined as adipose tissue directly surrounding blood vessels without separation from the adventitia [10], modulates vascular function in an endocrine and/or paracrine manner [10, 11]. Under physiological conditions, PVAT attenuates vasoconstriction induced by contractile agonists, such as norepinephrine and phenylephrine (PE). This action has been referred to as an anti-contractile function of PVAT[12]. PVAT also augments vasorelaxation induced by vasodilators, including acetylcholine (ACh) [13, 14]. Mechanisms underlying the ability of PVAT to attenuate vasoconstriction and augment vasorelaxation include secretion of adipocyte-derived relaxing factors (ADRFs), such as adiponectin [15], hydrogen sulfide (H_2S)[16] and nitric oxide (NO)[17]. The various ADRFs are thought to act on potassium channels in vascular smooth muscle cells to elicit anti-contractile response, and also act on endothelial cells to enhance nitric oxide (NO) mediated vasorelaxation [18, 19]. In obese murine models, both the anti-contractile properties [14, 20] and ability of PVAT to augment vasorelaxation [14] are impaired. In the case of impaired anti-contractile actions in response to norepinephrine, it has been suggested that this impairment relates to overproduction of TNF-α and IL-6 in PVAT [2]. Further, the impaired ability of PVAT to augment vasorelaxation in obesity can be partially restored by application of soluble adiponectin which enhances NO production by endothelial cells [14].

Dendritic cells are professional antigen presenting cells that participate in immune system surveillance and maintenance [21]. Further, these cells have been suggested to contribute to tissue inflammation independent of their antigen presenting function [22, 23]. Defects in dendritic cell function have been shown to be involved in a number of pathological states including cancer[24], immunodeficiency and autoimmune diseases[25, 26], atherosclerosis[27], and type 1 diabetes[28]. Amongst a number of studies reporting roles for dendritic cells in adipose tissue[29], it has also been shown that in obesity dendritic cells show enhanced secretion of inflammatory cytokines, including transforming growth factor beta (TGF_{β}) into adipose tissue [30]. We therefore posited that dendritic cells would accumulate in PVAT and produce inflammatory cytokines, which subsequently contribute to the impaired anti-contractile and vasorelaxation responses caused by chronic inflammation in a murine model of T2DM. Consistent with this hypothesis, our findings revealed that dendritic cells do accumulate in PVAT and visceral adipose tissue (VAT) of T2DM mice and enhance production of pro-inflammatory cytokines in obese adipose tissue. The data provide strong and novel evidence for an increased presence of dendritic cells underlying impairment of anti-contractile and vasodilator activities in PVAT of the T2DM mice, suggesting an important role for these immunocytes in vascular dysfunction in T2DM.

2. Methods

2.1 Animals

All procedures and protocols involving mice were approved by the Laboratory Animal Care Committee at University of Missouri, Columbia, Missouri, USA. Homozygote T2DM mice (*Lepr*^{db}, *db/db* mice) and heterozygote controls (m *Lepr*^{db}, DbHET mice) on the same C57BLKS/J strain were purchased from Jackson Laboratory. Flt3l$^{-/-}$ mice, which were used as a murine model depleted of dendritic cells were purchased from Taconic Farm [31]. To obtain T2DM mice depleted of dendritic cells, we cross-bred Flt3l$^{-/-}$ with DbHET mice for two generations. DbHET$^{Flt3l-/-}$ and *db*$^{Flt3l-}$/*db*$^{Flt3l-}$ mice were subsequently obtained by breeding of the heterozygote mice. All mice were housed in a pathogen-free animal facility and maintained in a constant temperature and humidity environment on a 12-hour light/dark switch per day. Mice had ad libitum access to water and a standard chow diet. All mice were anesthetized with nembutal (65mg/kg)[32] and euthanized under anesthesia.

2.2 Metabolic determinations

Body weight and weights of mesenteric adipose tissue (MAT), visceral adipose tissue (VAT), peri-aortic adipose tissue (ATA), pericardial adipose tissue (AH) were recorded. Non-fasting blood glucose levels were measured using a ReliOn prime blood glucose monitoring system. For glucose tolerance tests, mice were deprived of food overnight for approximately 16 hours while for insulin tolerance tests, mice were fasted for 4 hours. After fasting, tail tips were cut with sterile scissors and baseline glucose levels measured. 20% glucose solution or 0.5 U/kg insulin (Humalin® R; Eli Lilly) volume [33] were given intraperitoneally. Blood glucose levels were measured at 0, 30, 60, 90, and 120 minutes.

2.3 Isolation of Stromal Vascular Fraction Cells from Adipose Tissue

VAT was collected from DbHET, *db/db*, DbHET $^{Flt3l-/-}$ and db^{Flt3l-}/db^{Flt3l-} mice and using sterile scissors minced into fine particles (<10 mg) in freshly made solution containing 1× Phosphate Buffered Saline (PBS) (Ca/Mg^{2+} free)(Gibco Company, Waltham, MA, USA), 0.5% bovine serum albumin (Sigma Company, Cream Ridge, NJ, USA) and 10mM $CaCl_2$ [34]. 2 mg/ml type II collagenase (Sigma Company, Cream Ridge, NJ, USA) was added to the above solution and shaken at 37° C for 20 minutes. Subsequently 1 mM EDTA was applied to stop the collagenase activity and the solution passed through 100-μm nylon strainers to remove undigested adipose tissue. The suspension was then centrifuged at 1600 rpm for 5 minutes at room temperature. The resultant pellet was considered the stromal vascular fraction and then re-suspended in erythrocyte lysis buffer (Biolegend Company, San Diego, CA, USA). After erythrocytes were removed, the remaining cells were re-suspended in 1× PBS without Ca^{2+} or Mg^{2+} for flow cytometry analysis.

2.4 Flow Cytometry Analysis

After determination of cell number and viability of the erythrocyte-depleted stromal vascular cells, the preparation was washed (×2) with flow cytometry staining buffer (Ebioscience Company, San Diego, CA, USA). 1 μg/ml Fc-blocker (Sigma Company, Cream Ridge, NJ, USA) was added into cell suspension to avoid non-specific binding of the primary antibodies. Following incubation at 4 °C for 15 minutes in the dark, cells were treated with 1:200 dilution of anti-CD11c antibody(BD Pharmingen Company, San Jose, CA, USA), anti-CD83 antibody (Biolegend Company, San Diego, CA, USA) and anti-CD86 antibody(Ebioscience Company, San Diego, CA, USA) as well as 1:400 dilution of anti-F4/80 antibody(Ebioscience Company, San Diego, CA, USA) and incubated for a further 45 minutes in the dark. After washing with flow cytometry staining buffer (×2), cells were measured using a CyAn ADP High-Performance Flow Cytometer and Summit software [35]. The final data were obtained using Flowjo software. The dendritic cell population was identified as $CD11c^+F4/80^-$ and $CD83^+CD86^+$ cell populations whereas macrophage was identified as the $CD11c^+F4/80^+$ cell population.

2.5 mRNA measurements

After mice were anesthetized, VAT, MAT, ATA, AH, first or second order mesenteric arteries (MA), thoracic aorta (TA) and left anterior descending coronary artery (LAD) were dissected and snap frozen in liquid N_2 for subsequent mRNA analysis using real-time quantitative polymerase chain reaction (qPCR) measurements. Total RNA was extracted from VAT, MAT, ATA and AH using RNeasy lipid tissue mini kits (Qiagen Company, Valencia, CA, USA). Total RNA was extracted from spleen using a RNeasy mini kit (Qiagen Company, Valencia, CA, USA). Total RNA was extracted from MA and LAD using Arcturus Pico Pure RNA isolation kit (Life Technologies Company, Grand Island, NY, USA) while TA total RNA was prepared using a RNeasy fibrous tissue mini kit (Qiagen Company, Valencia, CA, USA). Quality and quantity of RNA were measured using a Nano Drop ND-1000 Spectrophotometer (Nano Drop Technologies, Wilmington, DE). cDNA was reverse transcribed using a SuperScript III First-Strand Synthesis System (Invitrogen Company, Grand Island, NY, USA). Amplification of cDNA was performed using a

Platinum® SYBR® Green qPCR SuperMix-UDG (Invitrogen Company, Grand Island, NY, USA) in an iQ5 Real-Time PCR system (Biorad company, Hercules, CA, USA). The housekeeping gene glyceraldehyde 3-phosphate dehydrogenase (GAPDH) was used for internal normalization. Spleen cDNA from a male DbHET mouse at 12 weeks was used as a calibrator. Primers were as follows: CD11c: Forward: ctggatagcctttcttctgctg; Reverse: gcacactgtgtccgaactca. GAPDH: Forward: aatggtgaaggtcggtgtg; Reverse: gtggagtcatactggaacatgtag. TNF-α: Forward: gtccccaaagggatgagaag; Reverse: cacttggtggtttgctacga. IL-6: Forward: ccggagaggagacttcacag; Reverse: tccacgatttcccagagaac. Adiponectin: Forward: gtctcacccttaggaccaagaa; Reverse: aggttggatggcaggc. IL-10: Forward: atggccttgtagacaccttg; Reverse: gtcatcgatttctcccctgtg. The mean threshold cycle (CT) values were calculated by the $2^{-\Delta\Delta CT}$ method ($\Delta\Delta CT=C_{T.CD11c}-C_{T.GAPDH}$) [36]. Results are presented as fold change of transcripts for CD11c normalized to GAPDH, compared with the calibrator (defined as 1.0 fold). mRNA levels of TNF-α, IL-6, adiponectin and IL-10 were presented as fold change of transcripts for the various inflammatory cytokines normalized to GAPDH.

2.6 Immunohistochemistry

VAT was fixed in 10% formalin (Sigma Company, Cream Ridge, NJ, USA) for 18-24 hours. Samples were then embedded in paraffin and cut into 5 μm thick sections [37]. Sections were then de-paraffinized with using a series concentration of xylene and ethanol. Following antigen retrieval steps, VAT sections were incubated with blocking goat serum at room temperature for 1 hour to prevent nonspecific binding of the primary antibodies. VAT sections were then incubated overnight with hamster anti-mouse CD11c primary antibodies (1:200 dilution, Abcam Company, Cambridge, United Kingdom) at 4°C. After washing with TBS (Tris-Buffered Saline), VAT sections were incubated at room temperature for 3 hours with goat anti-hamster secondary antibodies conjugated with Texas-Red (1:1000 dilution, Abcam Company, Cambridge, United Kingdom). Nuclei were identified by DAPI (4′,6-diamidino-2-phenylindole) staining (Invitrogen, Carlsbad CA, USA). The fluorescence staining was then visualized under an Olympus microscope (model IX81). To evaluate the infiltration of $CD11c^+$ cells in VAT, adipocytes and $CD11c^+$ cells were counted from 10 random high power (×200) fields for each section [38, 39]. Six sections were collected from each mouse [39]. The percentage of $CD11c^+$ cells for each sample was determined as the sum of the number of CD11c-expressing cells divided by the total number of surrounding adipocytes in each field of view.

2.7 Assessment of mesenteric artery vasomotor function

After induction of anesthesia the small intestinal mesentery bed was quickly excised and placed in cold and freshly prepared physiological saline solution (PSS). PSS was composed of 4.69 mM KCl, 118.99 mM NaCl, 2.50 mM $CaCl_2$•$2H_2O$, 1.18 mM KH_2PO4, 1.17 mM $MgSO_4$•$7H_2O$, 14.9 mM $NaHCO_3$, 5.5 mM D-Glucose, and 0.03 mM EDTA. First order MA from DbHET, *db/db*, DbHET $^{Flt3l-/-}$ and db^{Flt3l-}/db^{Flt3l-} mice at 6-10 or 18-22 weeks of age, were dissected and cleaned of adherent tissue before being cut into rings approximately 2mm in width. Approximately 0.5 gram of surrounding MAT was saved in PSS for co-incubation experiments. MA rings were carefully positioned between 2 stainless steel wires (diameter 17 μm) in organ chambers of an isometric wire myograph (DMT

610M, A&D Instruments) [40]. Tension was applied to the MA rings to approximate a transmural pressure of 100 mmHg. Passive length-tension relationships were determined for each MA ring. During experiments, the circumference of MA rings was maintained constant and responses were examined under isometric conditions. All MA rings were maintained at 37° C in PSS aerated continuously with 95%air–5%CO_2 [41]. After 30 minutes equilibration, MA rings were first challenged with 80mmol/L potassium chloride and this procedure was repeated for 3 times until a constant constriction response was achieved. Subsequently, endothelium-dependent relaxation responses to Ach, and contractile responses to PE, were determined in a cumulative dose-dependent manner (10^{-9}—10^{-5} mol/L). PE-induced vasoconstriction response was expressed as a percentage of the contraction to 80mmol/L potassium chloride whereas ACh-induced relaxation responses were calculated as a percentage of PE (1×10^{-5} mol/L)-induced pre-constriction. In MAT co-incubation protocols, 0.5g MAT was directly placed in the same organ chamber containing one MA ring for 1 hour, which was termed as “MAT incubation”. MA rings mounted in an organ chamber and not incubated with MAT, acted as “time controls”. After the 1 hour incubation, PE-induced vasoconstriction and ACh-induced vasorelaxation responses were again examined to determine whether MAT incubation affected vascular function. In order to test whether any MAT-induced effects could be washed out, PE-induced vasoconstriction and ACh-induced relaxation responses were repeated after MA rings were washed every 10 minutes with PSS for 1 hour.

2.8 MAT transfer bioassay experiments

Basic protocols were similar to those used in the above functional assessment experiments. In these experiments, MA from DbHET mice at 18-22 weeks were isolated and mounted in organ chambers. MAT from the same DbHET mice was saved in PSS for following steps. MAT from *db/db* mice at 18-22 weeks was also collected and similarly saved in PSS. After recording baseline ACh-induced vasorelaxation and PE-induced vasoconstrictor responses in the absence of MAT, one MA ring from DbHET mouse was co-incubated with 0.5g MAT from the same DbHET mouse, while a second MA ring from the DbHET mouse was co-incubated with 0.5g MAT from a *db/db* mouse. An additional, MA ring from DbHET mouse without MAT co-incubation was used as sham or time control. Following 1hour co-incubation, vasomotor responses were repeated to determine the effects of MAT on vascular function. Similarly, MA rings from DbHET$^{Flt3l-/-}$ mice at 18-22 weeks were mounted in organ chambers and separated into three groups - including DbHET$^{Flt3l-/-}$ MAT incubation; db^{Flt3l-}/db^{Flt3l-}; MAT incubation and time control. ACh-induced vasorelaxation and PE-induced vasoconstriction responses were again determined after a 1 hour MAT incubation. In all experiments vasomotor responses were again repeated after washout.

2.9 Statistical Analysis

All the results are expressed as mean ± standard error mean (SEM). In general, data were analyzed by one-way Analysis of Variance (ANOVA), along with Tukey’s multiple comparison post-test. For assessment of vascular function and MAT transfer bioassay data, two-way ANOVA was performed, along with Bonferroni post-test. $P < 0.05$ was considered statistically significant in all studies.

3. Results

3.1 Expression of CD11c mRNA levels on vasculature and PVAT

Dendritic cells and macrophages have been shown to be located in thoracic aorta (TA) tissue and to participate in inflammation associated with atherosclerosis [42, 43]. Further, accumulating evidence indicates that adipose tissue is an immunological organ harboring various immune cells, including inflammatory M1 macrophages [4, 44]. In order to identify the location of dendritic cells and macrophages in the db/db model of T2DM, we measured CD11c mRNA levels in several vascular locations and associated adipose tissue depots. TA, left anterior descending (LAD) and mesenteric artery (MA) were collected from both DbHET and *db/db* mice at 6-10, 12-16, 18-22 and > 24 weeks of age and CD11C mRNA expression levels measured by qPCR (Figure 1 A–C). Low levels of CD11c expression were detected in all vascular samples with no apparent differences observed between DbHET and *db/db* mice. Further, age-dependent differences in CD11c mRNA expression levels were not observed. In contrast, CD11c mRNA expression was significantly increased in visceral adipose tissue (VAT) (Figure 1D), MAT (Figure 1E), and peri-aortic adipose tissue (ATA) (Figure 1G) from *db/db* mice, in comparison with age-matched DbHET controls at all four age groups. CD11c mRNA levels in peri-cardiac adipose tissue (AH) (Figure 1F) were increased in *db/db* mice compared to DbHET mice only at 18- through 24 weeks groups. A general trend showed a duration of diabetes/age-dependent increase in adipose tissue CD11C mRNA expression levels in *db/db* mice while levels remained unchanged in DbHET mice across all four age groups. As shown in Figure 1H, at > 24 weeks of age, the majority of CD11c mRNA expression in *db/db* mice was located in VAT and MAT while CD11c levels in DbHET mice were similar across adipose tissue samples. On the basis of these findings, subsequent studies were focused on visceral and mesenteric adipose tissues.

3.2 Quantification of dendritic cells in VAT by flow cytometry analysis

To obtain an index of dendritic cell marker protein expression, we collected VAT samples from DbHET and *db/db* mice at 6-10 and 18-22 weeks of age and performed flow cytometry. To increase the specificity for identifying dendritic cells, two combinations of cell surface molecular markers were used: $CD11c^{+}F4/80^{-}$ and $CD83^{+}CD86^{+}$. The $CD11c^{+}F4/80^{+}$ cell population was considered as M1 macrophages. As shown in Figure 2, an approximately two fold increase in $CD11c^{+}F4/80^{-}$ dendritic cells (Figure 2A and B) and 2.5 fold increase in $CD83^{+}CD86^{+}$dendritic cells were present in VAT from *db/db* compared to DbHET mice at both 6-10 and 18-22 weeks (Figure 2C and D, **respectively**). Flow cytometry data did not, however, demonstrate age/duration of diabetes-dependent differences (Figure 2A–D). Similar to a diabetes-induced increase in dendritic cells, a greater than two fold increase in $CD11c^{+}F4/80^{+}$ M1 macrophages was detected in VAT from *db/db* in comparison with DbHET mice (Figure 2E and F). No significant change of M1 macrophage number was apparent between the 6-10 and 18-22 week groups in either *db/db* or DbHET mice (Figure 2E and F). Collectively, these flow cytometry results support the mRNA data suggesting that at the protein marker level, more dendritic cells and M1 macrophages were recruited into VAT from diabetic mice, compared to their normoglycemic and lean heterozygote controls.

3.3 Location of dendritic cells in VAT from diabetic mice

To determine the location of the dendritic cells within adipose tissue, immunohistochemistry was used to stain CD11c protein in VAT from *db/db* and DbHET mice (6-10 and 18-22 weeks of age). $CD11c^+$ cells were located within the stromal vascular fraction of VAT, surrounded by adipocytes, in both DbHET and *db/db* mice (Supplementary Fig. 1A). Further, more $CD11c^+$ cells infiltrated VAT in *db/db* compared to DbHET mice at both 6-10 and 18-22 weeks (Supplementary Figure 1B). Similar to the flow cytometry data, immunohistochemistry analysis did not show an age-dependent difference in the distribution of $CD11c^+$ cells in either DbHET or *db/db* mice.

3.4 Depletion of dendritic cells in db/db mice

$Flt3l^{-/-}$ mice have been reported to have very low levels of dendritic cells in adipose tissue, spleen and liver[45]. We, therefore, cross-bred $Flt3l^{-/-}$ with DbHET mice to generate DbHET$^{Flt3l-/-}$ and db^{Flt3l-}/db^{Flt3l-} mice, which were used as a diabetic model with a genetic deficiency of dendritic cells. To confirm that depletion of Flt3l removed dendritic cells without any effect on macrophages, VAT from DbHET, *db/db*, DbHET $^{Flt3l-/-}$ and db^{Flt3l-}/db^{Flt3l-} mice were collected at 6-10 weeks of age. Depletion of Flt3l significantly decreased $CD11c^+F4/80^-$ (Supplementary Figure 2C) and $CD83^+CD86^+$ dendritic cells (Supplementary Figure 3C) populations in VAT from DbHET $^{Flt3l-/-}$, compared to DbHET mice (Supplementary Figure 2A and 3A). Similarly, Flt3l depletion also dramatically decreased $CD11c^+F4/80^-$ (Supplementary Fig. 2D) and $CD83^+CD86^+$ dendritic cells (Supplementary Figure 3D) populations in VAT from db^{Flt3l-}/db^{Flt3l-} mice by approximately 3 to 5 fold, compared to *db/db* mice. The data also showed that $CD11c^+F4/80^-$ (Figure 3A) and $CD83^+CD86^+$ (Figure 3B) dendritic cells were comparable between DbHET $^{Flt3l-/-}$ and db^{Flt3l-}/db^{Flt3l-} mice. In contrast, Flt3l depletion did not significantly alter the number of $CD11c^+F4/80^+$ macrophages in either DbHET$^{Flt3l-/-}$ (Supplementary Figure 2C) or db^{Flt3l-}/db^{Flt3l-} mice (Supplementary Figure 2D). Consistent with the earlier data, a greater number of $CD11c^+F4/80^+$ macrophages infiltrated VAT from db^{Flt3l-}/db^{Flt3l-} in comparison with DbHET $^{Flt3l-/-}$ mice (Figure 3C). Collectively, genetic depletion of Flt3l significantly reduced dendritic cell numbers in VAT from DbHET $^{Flt3l-/-}$ and db^{Flt3l-}/db^{Flt3l-} mice, without having any influence on macrophage numbers. On the basis of these findings, DbHET $^{Flt3l-/-}$ and db^{Flt3l-}/db^{Flt3l-} mice were used in the following studies.

3.5 Effect of dendritic cells depletion on body weight, weights of adipose tissue depots and plasma glucose levels

Studies have demonstrated that ablation of $CD11c^+$ cells rapidly normalized insulin sensitivity in diet-induced obese mice [46, 47]. Further, earlier studies [45] have shown that $Flt3l^{-/-}$ mice display an increased metabolic rate and are protected against diet-induced obesity. It was therefore considered possible that DbHET $^{Flt3l-/-}$ and db^{Flt3l-}/db^{Flt3l-} mice in our study would similarly exhibit low glucose levels and high metabolic rate with low adipose tissue weights. To test this, non-fasting glucose levels, total body weight along with mesenteric bed, VAT, AH and ATA weights were measured in DbHET, *db/db*, DbHET$^{Flt3l-/-}$ and db^{Flt3l-}/db^{Flt3l-} mice at 6-10 and 18-22 weeks. As shown in Supplementary Figure 4, at 6-10 weeks of age, *db/db* mice showed increased total body weight, mesenteric bed weight,

VAT, AH and ATA weights, along with higher non-fasting glucose levels, than DbHET mice. Similar results were seen at in the older age groups (18-22 weeks, Figure 4). Depletion of dendritic cells did not alter those phenotypic parameters in either DbHET$^{Flt3l-/-}$ or db^{Flt3l-}/db^{Flt3l-} mice at 6-10 weeks of age, but did decrease mesenteric bed (Figure 4C) and VAT (Figure 4D) weights and non-fasting glucose levels (Figure 4B) in the db^{Flt3l-}/db^{Flt3l-} mice at 18-22 weeks. Glucose and insulin tolerance tests (Figure 4G and H), performed after a period of fasting, showed significantly lower blood glucose levels in db^{Flt3l-}/db^{Flt3l-} mice in comparison with *db/db* mice aged 18 – 22 weeks, indicative of partial restoration of insulin sensitivity.

3.6 Effects of dendritic cell depletion on on production of pro-inflammatory and anti-inflammatory factors in adipose tissue

Depletion of CD11c^{+} cells has previously been shown to lead to a marked reduction of inflammatory responses in both obese VAT and the systemic circulation [47]. This raised the question as to whether depletion of dendritic cells would also result in the reduction of chronic inflammation induced in the db/db model of T2DM. Therefore, we posited that depletion of Flt3l would significantly decrease pro-inflammatory cytokines and increase anti-inflammatory factors in adipose tissue db/db mice. To test this notion we used qPCR to measure pro-inflammatory factors TNF-α and IL-6, along with anti-inflammatory mediators adiponectin and IL-10 mRNA levels in VAT and MAT from DbHET, *db/db*, DbHET $^{Flt3l-/-}$ and db^{Flt3l-}/db^{Flt3l-} mice at both 6-10 and 18-22 weeks. At the younger age (6-10 weeks) mRNA levels for TNF-α and IL-6 were increased in VAT and MAT from *db/db* mice, compared to DbHET mice (Supplementary Figure 5). Depletion of dendritic cells significantly decreased TNF-α levels in VAT and MAT from db^{Flt3l-}/db^{Flt3l-} mice, while IL-6 mRNA levels were decreased in MAT but not in VAT (Supplementary Figure 5 A–D). mRNA levels of adiponectin were decreased in the VAT from *db/db* mice, compared to controls while depletion of dendritic cells did not restore adiponectin production in db^{Flt3l-}/db^{Flt3l-} mice (Supplementary Figure 5E). At the younger age, mRNA levels of adiponectin in MAT, along with IL-10 in VAT and MAT, were similar in *db/db* and DbHET mice. Depletion of dendritic cells still did not affect these patterns (Supplementary Figure 5F–H). At the later stage of T2DM (18-22 weeks), mRNA levels for TNF-α and IL-6 were increased in VAT and MAT from *db/db* mice, compared to controls (Figure 5). Dendritic cell depletion significantly reduced TNF-α and IL-6 levels in VAT and MAT from db^{Flt3l-}/db^{Flt3l-} mice (Figure 5A–D). In contrast, mRNA levels of adiponectin were decreased in VAT and MAT from *db/db* mice, compared to controls (Figure 5E, F) and were not restored by dendritic cell depletion Interestingly, IL-10 mRNA levels were increased in VAT and MAT from *db/db* mice, compared to controls (Figure 5G, H). Dendritic cell depletion significantly reduced IL-10 levels only in MAT from db^{Flt3l-}/db^{Flt3l-} mice. (Figure 5H). Collectively, depletion of dendritic cells attenuated chronic inflammation in db/db mice as evidenced by a reduced production of pro-inflammatory factors TNFα and IL-6.

3.7 Effect of MAT on vascular reactivity in DbHET and db/db mice

Under physiological conditions PVAT, such as that in MAT, elicits an anti-contractile action on the vasculature [12, 48]. To examine this in our model we first isolated first order MA segments from DbHET mice (6-10 and 18-22 weeks of age) and divided them into two

groups: one group acting as a time control (sham) in the absence of adipose tissue and the other incubated in the presence of MAT (taken from the same animal group). Both groups were exposed to cumulative concentrations of ACh or PE before MAT (or sham) incubation, after 1 hour MAT incubation and again after a 1 hour wash period. At 6-10 weeks of age, a 1 hour incubation of MA with MAT from DbHET mice significantly enhanced ACh induced vasorelaxation (Figure 6A) with a significant difference in logEC50 values between sham and MAT exposed MAs (Supplemental Table 1). In addition, incubation of MAs with MAT significantly attenuated PE-induced vasoconstriction (Figure 6C). Significant differences in logEC50 values for PE between time control and MAT incubation further confirmed the anti-contractile property of MAT from DbHET mice (Supplemental Table 1). Similar results were found in DbHET mice at 18-22 weeks (Supplementary Figure 6). Importantly, the effects mediated by MAT were reversed by MAT removal and replacing the incubation media.

Previous reports have shown that the anti-contractile function of PVAT is impaired in obese animal models [14, 49]. Further, in *db/db* mice, insulin-induced vasodilation of resistance arteries of skeletal muscle was diminished by the presence of PVAT [14]. To extend these observations similar protocols to the above were used to examine the effect of MAT from db/db mice on MA reactivity. At 6-10 weeks of age MAT from db/db mice failed to enhance ACh-induced vasorelaxation (Figure 6B) or attenuate PE- induced vasoconstriction (Figure 6D). Similarly, logEC50 values were similar between MA incubated with and without MAT from db/db mice (Supplemental Table 1). A similar inability of MAT to modulate vasomotor responses in *db/db* mice was also observed at 18-22 weeks of age (Supplementary Figure 7).

3.8 Effect of MAT on vascular reactivity in DbHET $^{Flt3l-/-}$ and db^{Flt3l-}/db^{Flt3l-} mice

To determine whether dendritic cell depletion restored the vasoactive properties of PVAT similar vascular function studies were performed in DbHET $^{Flt3l-/-}$ and db/db $^{Flt3l-/-}$ mice. At 6-10 weeks of age a 1 hour incubation of MA segments with MAT from DbHET $^{Flt3l-/-}$ significantly enhanced Ach-induced vasorelaxation (Figure 7A) and attenuated PE-induced constriction (Figure 7C). Further, significant differences in logEC50 values for both ACh and PE concentration curves were observed between time control and MAT incubations (Supplemental Table 1). A 1hour wash with fresh buffer again abolished the differences between time control (sham) and MAT incubations with a similar pattern of results being observed in DbHET $^{Flt3l-/-}$ mice (Supplementary Figure 8).

In contrast to the data obtained in db/db mice, a 1hour incubation of MA with adipose tissue from *db*$^{Flt3l-}$/*db*$^{Flt3l-}$ mice (6-10 weeks of age) significantly enhanced ACh-induced vasorelaxation (Figure 7B) and attenuated PE-induced vasoconstriction responses (Figure 7D). Consistent with this, logEC50 values obtained for ACh and PE concentration curves showed significant differences between sham and MAT incubations (Supplemental Table 1). A 1hour wash with fresh buffer abolished the differences between sham and MAT incubations (Supplementary Figure 10). At 18-22 weeks, MAT from *db*$^{Flt3l-}$/*db*$^{Flt3l-}$mice significantly enhanced ACh induced vasorelaxation (Supplementary Figure 9 B) but did not impact PE-induced vasoconstriction responses (Supplementary Figure 9 F). Collectively, at the earlier stage of T2DM, MAT from *db*$^{Flt3l-}$/*db*$^{Flt3l-}$ both augmented vasorelaxation

responses and exhibited anti-contractile activity, while at the later stage of T2DM, MAT from *db*$^{Flt3l-}$/*db*$^{Flt3l-}$ mice only maintained PVAT effects on vasorelaxation responses.

3.9 MAT transfer assay between DbHET and db/db mice (18-22 weeks of age)

To further confirm that the impaired vascular reactivity in *db/db* mice was due to dysfunction of the adipose tissue, we conducted a series of 'MAT transfer assays'. Using first order MA from DbHET mice, ACh-induced vasorelaxation was enhanced when incubated with MAT from the same mice (Figure 8A), consistent with the earlier data shown in Figure 6. In contrast, when MAs from DbHET mice were acutely (1hr) incubated with MAT from *db/db* mice the augmentation of ACh-induced vasorelaxation was abolished (Figure 8A). Similarly, PE-induced vasoconstriction was attenuated when MA from DbHET were incubated with their own MAT (Figure 8B). In contrast, when MAs were incubated with MAT from *db/db* mice, this reduction of vasoconstriction was markedly attenuated. Collectively the data suggest that MAT from the *db/db* mice creates an environment that impairs the normal augmentation of ACh-induced vasorelaxation and attenuated PE-induced vasoconstriction that occurs in the presence of control/non-diabetic adipose tissue.

3.10 MAT transfer assay between DbHET$^{Flt3l-/-}$ and db^{Flt3l-}/db^{Flt3l-} mice at 18-22 weeks

Similar transfer assays were conducted to determine whether MAT incubation from *db*$^{Flt3l-}$/*db*$^{Flt3l-}$ mice would affect vasomotor function of normal vessels. MA from DbHET$^{Flt3l-/-}$ mice were incubated with MAT from either DbHET$^{Flt3l-/-}$ or *db*$^{Flt3l-}$/*db*$^{Flt3l-}$ mice. MA incubated with MAT from DbHET$^{Flt3l-/-}$ mice exhibited a significant enhancement of ACh-induced vasorelaxation and a reduction of PE-induced vasoconstriction compared to a time control group (Figure 9A). In contrast to MAT from *db/db* mice, MAT from *db*$^{Flt3l-}$/*db*$^{Flt3l-}$ mice caused a similar enhancement of ACh-induced vasorelaxation and a comparable reduction in PE-induced vasoconstriction responses with MAT from DbHET$^{Flt3l-/-}$ mice (Figure 9B). LogEC50 values similarly indicated comparable vasorelaxation and vasoconstriction response curves for MA incubated with MAT from either DbHET$^{Flt3l-/-}$ and *db*$^{Flt3l-}$/*db*$^{Flt3l-}$ mice (Supplemental Table 1). Thus, while MAT from *db/db* mice markedly attenuates the normal augmentation of vasorelaxation and anti-contractile effects exerted by adipose tissue, genetic depletion of dendritic cells restores the ability of MAT to appropriately modulate vasomotor responses.

4. DISCUSSION

The present investigation was designed to determine the contribution of dendritic cells to the chronic inflammation and vascular dysfunction that is observed in obesity and T2DM. To undertake this, a novel murine model of T2DM depleted of dendritic cells, *db*$^{Flt3l-}$/*db*$^{Flt3l-}$ mouse, was developed. Key findings were: (1) In this obese T2DM murine model dendritic cells accumulated in adipose tissue rather than in the walls of adjacent arteries. (2) Dendritic cells promoted production of pro-inflammatory factors in adipose tissue from *db/db* mice. (3) The ability of adipose tissue to potentiate vasorelaxation and attenuate vasoconstriction was impaired at both early (6 - 10 weeks) and later (18 - 22 weeks) stages of T2DM. (4) Dendritic cell depletion decreased the inflammatory environment and restored the ability of PVAT to positively affect vascular function.

4.1 Dendritic cell expression in a murine model of T2DM

Previous studies have shown that CD11c+ dendritic cells [50, 51] and M1 macrophages [52, 53] accumulate in atherosclerotic lesions of the aorta and promote the further development of atherosclerosis and associated events such as plaque rupture. In obesity/T2DM, M1 macrophages accumulate in various adipose tissue sites and potentiate the development of chronic inflammation as well as promotion of insulin resistance [54, 55]. It is acknowledged that atherosclerosis and diabetes share similar pathological processes, including chronic low grade inflammation [56, 57]. We therefore first ascertained whether $CD11c^{+}$cells, including dendritic cells, accumulated in either the vasculature or PVAT, or at both locations during the progression of T2DM. Our qPCR data (Figure 1) showed that only low levels of CD11c mRNA were found in arteries taken from multiple vascular beds of both diabetic and heterozygous control mice. In contrast, higher levels of CD11c mRNA expression (compared to the same calibrator used for the vessel wall studies) were detected in all PVAT and VAT samples from both diabetic and control mice. Diabetic mice, however, showed markedly higher adipose tissue CD11c mRNA levels at all ages studied. Similarly, flow cytometry data (Figure 2) (using $CD11c^{+}F4/80^{-}$ and $CD83^{+}CD86^{+}$ as complementary dendritic cell marker sets) showed accumulation of dendritic cells in the stromal vascular fraction with this occurring at a higher level in diabetic adipose tissue compared to that of non-diabetic mice. Based on these findings, it appears that in the db/db model of T2D dendritic cells are recruited to the stromal vascular fraction of adipose tissue, i.e. PVAT, as opposed to within the vascular wall.

4.2 Depletion of dendritic cells in a murine model of T2DM

To provide a model of dendritic cell depletion we used $Flt3l^{-/-}$ mice [45] cross-bred with DB/db heterozygote mice. Flt3l (ligand for FMS-like tyrosine kinase 3) is a growth factor for hematopoietic progenitor cells in mice [58]. A lack of Flt3l has been reported to reduce dendritic cell number in murine lymphoid organs[58]. This approach was chosen instead of the use of CD11c-DTR (diphtheria toxin receptor) transgenic mice[47, 59] as it relies on a molecular genetic approach to deplete dendritic cells, that does not require chemical administration (i.e. diphtheria toxin). More importantly, the Flt3I knockout mouse remains depleted of dendritic cells, making it suitable for longitudinal studies of T2DM, whereas the CD11c-DTR model requires repeated diphtheria toxin injections over time to maintain low dendritic cell numbers. Flow cytometry data (Supplementary Figure 2) confirmed that these mice exhibited markedly reduced $CD11c^{+}F4/80^{-}$ and $CD83^{+}CD86^{+}$ cell populations in VAT with normal levels of M1 macrophages. Further, Flt3l depletion, dramatically decreased dendritic cell numbers in db^{Flt3l-}/db^{Flt3l-} mice compared to *db/db* mice. Similar to control animals, Flt3l depletion did not significantly impact $CD11c^{+}F4/80^{+}$ M1 macrophage numbers in db^{Flt3l-}/db^{Flt3l-} mice compared to *db/db* mice. On the basis of these data it was concluded that $DbHET^{Flt3l-/-}$ and db^{Flt3l-}/db^{Flt3l-} mice provide an appropriate murine model to study the effects of dendritic cells on vascular dysfunction associated with T2DM.

4.3 Metabolic effects of dendritic cell depletion

As expected db/db mice exhibited increased body weights as well as increased weight of adipose depots (mesenteric bed, VAT, MAT, AH and ATA) and higher non-fasting glucose

levels compared to healthy mice at both early and later stages of T2DM (Supplementary Figure 4 and Figure 4). Depletion of dendritic cells decreased mesenteric bed and VAT weights, as well as non-fasting glucose levels in diabetic mice at 20 weeks of age whereas dendritic cell depletion did not affect these parameters in the younger diabetic mice. Previous studies in insulin resistant mice have reported that ablation of $CD11c^{+}$ cells can normalize glucose homeostasis and insulin responsiveness by correction of the inflammatory environment [47]. Consistent with this notion, current qPCR data (Figure 5 and Supplementary 5) showed that dendritic cell depletion significantly reduced the production of pro-inflammatory factors TNF-α and IL-6 in adipose tissue of the diabetic mice. Further, glucose levels and insulin responsiveness improved in db^{Ftl3l-}/db^{Ftl3l-} mice although glucose levels remained significantly higher than in healthy controls (Figure 4 G–H). These results suggest that dendritic cells may contribute to the development of high glucose levels and insulin resistance in *db/db* mice. That being said future studies should also examine, in this model, the roles of ectopic fat in liver and muscle as well as altered leptin signaling in the metabolic abnormalities in db/db mice. Further, the data do not preclude a role for other immune cells, such as increased PVAT M1 macrophages, which could also promote insulin resistance and associated glucose elevations.

While mesenteric bed and VAT weights were decreased in diabetic mice after dendritic cell depletion they remained higher than that observed in normoglycemic controls. Interestingly, $Flt3l^{-/-}$ mice have been reported [45] to exhibit higher metabolic rates than wild type mice. It is therefore conceivable that db^{Ftl3l-}/db^{Ftl3l-} mice maintain this high metabolic rate and as a result show a reduction in adipose tissue accumulation. However, increased numbers of pro-inflammatory M1 macrophages were apparent in adipose tissue of db^{Ftl3l-}/db^{Ftl3l-} mice (Figure 3C). As M1 macrophages have been shown to disrupt insulin-stimulated glucose transport and cause hypertrophy of adipose tissue[60] this may also partially explain why mesenteric bed and VAT weights remained higher in db^{Ftl3l-}/db^{Ftl3l-} mice compared to controls.

4.4 Adipose tissue inflammation in db/db mice: effect of dendritic cell depletion

Our data are consistent with a chronic inflammatory response in adipose tissue of db/db mice which is evident from an early age (6 – 10 weeks of age). Thus, in db/db mice mRNA levels for the pro-inflammatory factors, TNF-α and IL-6, were increased in VAT and MAT while mRNA for the anti-inflammatory mediator, adiponectin, was decreased in VAT. In contrast, at this young age, mRNA levels for adiponectin in MAT along with those for the anti-inflammatory mediator IL-10 in VAT and MAT were not affected. Dendritic cell depletion in T2DM mice (db^{Ftl3l-}/db^{Ftl3l-}) significantly decreased TNF-α mRNA levels in VAT and MAT, as well as IL-6 mRNA levels in MAT, without influence on adiponectin and IL-10 mRNA levels. The severity of adipose tissue inflammation increased with the duration and progression of T2DM such that in db/db mice, at 18-22wks of age, TNF-α and IL-6 mRNA levels were progressively increased while adiponectin mRNA levels were decreased in VAT and MAT. Interestingly, IL-10 mRNA levels were increased in VAT and MAT from bb/db mice. In this older group, dendritic cell depletion significantly decreased mRNA levels of TNF-α and IL-6 in VAT and MAT, as well as IL-10 in MAT. As previous studies [61, 62] have shown IL-10 to be a compensatory cytokine, which suppresses the production of pro-

inflammatory factors, including TNF-α and IL-6, this compensatory immune response could explain the apparent increase of IL-10 production in adipose tissue from diabetic mice compared to healthy controls. Consistent with this, dendritic cell depletion decreased the production of TNF-α and IL-6 in diabetic adipose tissue while also causing a reduction in IL-10 production. Collectively, dendritic cell depletion significantly decreased production of pro-inflammatory factors in diabetic PVAT, resulting in attenuation of chronic inflammation.

4.5 PVAT and vascular function in db/db mice – effects of dendritic cell depletion

It is widely accepted that PVAT exerts an important influence on vascular function via paracrine and/or endocrine mechanisms [63, 64]. Under physiological conditions in lean animals, PVAT produces a number of vasoactive molecules, including adiponectin, H_2S and NO. These factors act to promote vasorelaxation and reduce vasoconstriction [64, 65], the latter being termed as an “anti-contractile” function of adipose tissue. Recent studies have shown that the anti-contractile action of adipose tissue is lost in obese mice [48, 49] and that in a high fat diet-induced obesity model PVAT paradoxically promotes vasoconstriction [66]. This change in vasomotor activity may relate to a pro-inflammatory environment as treatment of healthy PVAT with TNF-α, IL-6 or an antagonist of adiponectin reduces vasodilation of adjacent arteries. [2] Since our qPCR data (Figure 5 and Supplementary Figure 5) showed increased TNF-α and IL-6 production along with decreased adiponectin in VAT and MAT from *db/db* mice compared to DbHET controls, it was considered likely that *db/db* mice would exhibit impaired vascular function. Supporting this, incubation of MA with MAT from DbHET mice augmented vasorelaxation and anti-contractile activity (Figure 6 and Supplementary Figure 7), whereas these effects were not apparent when arteries were incubated with MAT from *db/db* mice (both 6-10 and 18-22 weeks of age) (Figure 6 and Supplementary Figure 7). As the impairment in vasorelaxation and anti-contractile activity in *db/db* mice could be attributable to either MAT dysfunction or vasculature damage, ‘MAT transfer assays’ were conducted (Figure 8). Incubation of a healthy ‘donor’ vessel with MAT from *db/db* mice resulted in impaired vasorelaxation and enhanced vasoconstriction compared to MAT from DbHET mice. Consistent with other studies [13, 14] these data suggest that dysfunction of MAT, per se, contributes to impaired vasorelaxation and anti-contractile activity in *db/db* mice. As this effect of MAT was observed after only 1 hour exposure of a healthy donor vessel to diabetic adipose tissue it is likely that this reflects loss of PVAT factors promoting vasodilation or the production of inflammatory factors which favor vasoconstriction in T2DM.

As outlined above dendritic cell depletion significantly reduced TNF-α and IL-6 production in VAT and MAT from *db/db* mice. Consistent with the qPCR data, dendritic cell depletion augmented vasorelaxation and anti-contractile properties of adipose tissue in *db/db* mice at 6-10 weeks, while only improving vasorelaxation at 18-22 weeks (Figure 9). This may reflect the progressive nature of diabetes in this animal model as despite improvement in metabolic state in dendritic cell depleted mice as they remained significantly obese and hyperglycemic compared with controls. Alternatively, the impaired anti-contractile function at the later time-point in dendritic cell depleted mice may result from vascular changes as in this protocol adipose tissue was incubated with vessel segments taken from the same animal. Further, dendritic cell depletion did not prevent the accumulation of other inflammatory cells

such as M1 macrophages. In experiments where MAT was collected from db^{Ftl3l-}/db^{Ftl3l-} mice (18-22 weeks of age) and incubated with healthy donor vessels, vasorelaxation and anti-contractile activity were similar to that observed when MAT was taken from $DbHET^{Flt3l-/-}$ mice (Figure 9). Overall, dendritic cell depletion improved both the inflammatory environment within adipose tissue of db/db mice and rescued vasorelaxing/anti-contractile actions of PVAT. Further studies are required to establish more definitive mechanistic links between these events.

Limitations and Future Directions—The results of the present investigation provide an association between peri-vascular adipose tissue dendritic cell accumulation, pro-inflammatory cytokine production and vascular dysfunction in the db/db model of T2D. This investigation did not differentiate dendritic cell subsets nor ascertain whether such cells directly give rise to the inflammatory environment and vascular dysfunction. Clearly, other cell types, including the observed increase in M1 macrophages are likely to contribute. In addition, the studies do not elucidate the factors that cause the accumulation of dendritic cells within the stromal vascular fraction of the various adipose tissue depots in T2DM. The acute actions of MAT observed in the transfer assays and the washout studies are suggestive of a role for secreted factors. Finally, while dendritic cell-induced vascular dysfunction is demonstrated (in terms of both vasodilation and vasoconstriction) in T2DM mice, more in depth studies are required to isolate the contributions of endothelial cells, vascular smooth muscle cells and vasoactive factors produced by peri-vascular adipose tissue. A further caveat on our interpretations relates to the observation that dendritic cell depletion (db^{Ftl3l-}/db^{Ftl3l-} model) while improving vascular function also caused a partial improvement in metabolic state. Nonetheless, our studies do provide evidence for a role for dendritic cells in diabetes-induced vascular dysfunction and add mechanistic information regarding the roles played by these cells in diabetes [22].

In summary, the present investigation demonstrates that in the db/db murine model of T2D dendritic cells accumulate in PVAT as opposed to within the walls of the vasculature. Associated with this accumulation, both an elevated production of pro-inflammatory cytokines and reduced production of anti-inflammatory factors were evident in VAT and mesenteric artery PVAT from *db/db* mice compared to controls. This imbalanced production of pro-inflammatory versus anti-inflammatory factors correlated with abnormal vasoreactivity that is seen in T2DM. Depletion of dendritic cells in db^{Ftl3l-}/db^{Ftl3l-} mice was associated with reduced production of pro-inflammatory cytokines within adipose tissue and the novel finding that this dendritic cell depletion restored the ability of MAT to potentiate vasorelaxation and attenuate contractile responsiveness. Collectively, these findings suggest an important role for adipose tissue dendritic cells in the regulation of vascular function during the progression of T2DM. To our knowledge the data are amongst the first to demonstrate a role for adipose tissue dendritic cells in promoting vascular dysfunction in T2DM mice and provide a potential therapeutic target for the treatment of vascular complications in obesity-related diabetes.

Supplementary Material

Refer to Web version on PubMed Central for supplementary material.

Acknowledgments

Source of Funding

Studies were supported by funding from the NIH RO1HL085119 (MAH) and NIH RO1AA022108 (RJK).

Appendix A

Supplementary Data

Abbreviation

ACh	acetylcholine
ADRF	adipocyte-derived relaxing factor
AH	pericardial adipose tissue
ATA	peri-aortic adipose tissue
DTR	diphtheria toxin receptor
Flt3l	ligand for FMS-like tyrosine kinase 3
H_2S	hydrogen sulfide
IFN-γ	interferon-gamma
IL-6	interleukin 6
LAD	left anterior descending coronary artery
MA	mesentery artery
MAT	mesenteric adipose tissue
NO	nitric oxide
PE	phenylephrine
PVAT	perivascular adipose tissue
TA	thoracic aorta
T2DM	type 2 diabetes
TNF-α	tumor necrosis factor alpha
VAT	visceral adipose tissue

References

1. Nguyen DM, El-Serag HB. The epidemiology of obesity. Gastroenterol Clin North Am. 2010; 39(1):1–7. [PubMed: 20202574]

2. Greenstein AS, et al. Local inflammation and hypoxia abolish the protective anticontractile properties of perivascular fat in obese patients. Circulation. 2009; 119(12):1661–1670. [PubMed: 19289637]

3. Yang Q, et al. Serum retinol binding protein 4 contributes to insulin resistance in obesity and type 2 diabetes. Nature. 2005; 436(7049):356–62. [PubMed: 16034410]

4. Grant RW, Dixit VD. Adipose tissue as an immunological organ. Obesity (Silver Spring). 2015

5. Guilherme A, et al. Adipocyte dysfunctions linking obesity to insulin resistance and type 2 diabetes. Nat Rev Mol Cell Biol. 2008; 9(5):367–77. [PubMed: 18401346]

6. Winer DA, et al. B cells promote insulin resistance through modulation of T cells and production of pathogenic IgG antibodies. Nature medicine. 2011; 17(5):610–617.

7. Nishimura S, et al. CD8+ effector T cells contribute to macrophage recruitment and adipose tissue inflammation in obesity. Nature medicine. 2009; 15(8):914–920.

8. Huh J, et al. Crosstalk between Adipocytes and Immune Cells in Adipose Tissue Inflammation and Metabolic Dysregulation in Obesity. Molecules and cells. 2014

9. Seijkens T, et al. Immune cell crosstalk in obesity: a key role for costimulation? Diabetes. 2014; 63(12):3982–3991. [PubMed: 25414012]

10. Eringa EC, Bakker W, van Hinsbergh VW. Paracrine regulation of vascular tone, inflammation and insulin sensitivity by perivascular adipose tissue. Vascular pharmacology. 2012; 56(5):204–209. [PubMed: 22366250]

11. Gu P, Xu A. Interplay between adipose tissue and blood vessels in obesity and vascular dysfunction. Rev Endocr Metab Disord. 2013; 14(1):49–58. [PubMed: 23283583]

12. Fernández-Alfonso MS, et al. Mechanisms of perivascular adipose tissue dysfunction in obesity. International journal of endocrinology. 2013; 2013

13. Wang H, et al. Obesity-induced endothelial dysfunction is prevented by deficiency of P-selectin glycoprotein ligand-1. Diabetes. 2012; 61(12):3219–27. [PubMed: 22891216]

14. Meijer RI, et al. Perivascular adipose tissue control of insulin-induced vasoreactivity in muscle is impaired in db/db mice. Diabetes. 2013; 62(2):590–8. [PubMed: 23048187]

15. Fesus G, et al. Adiponectin is a novel humoral vasodilator. Cardiovasc Res. 2007; 75(4):719–27. [PubMed: 17617391]

16. Wojcicka G, et al. Differential effects of statins on endogenous H2S formation in perivascular adipose tissue. Pharmacol Res. 2011; 63(1):68–76. [PubMed: 20969959]

17. Gao YJ, et al. Modulation of vascular function by perivascular adipose tissue: the role of endothelium and hydrogen peroxide. British journal of pharmacology. 2007; 151(3):323–331. [PubMed: 17384669]

18. Malinowski M, et al. Mechanisms of vasodilatatory effect of perivascular tissue of human internal thoracic artery. J Physiol Pharmacol. 2013; 64(3):309–16. [PubMed: 23959727]

19. Tano JY, Schleifenbaum J, Gollasch M. Perivascular adipose tissue, potassium channels, and vascular dysfunction. Arterioscler Thromb Vasc Biol. 2014; 34(9):1827–30. [PubMed: 25012133]

20. Agabiti-Rosei C, et al. Anticontractile activity of perivascular fat in obese mice and the effect of long-term treatment with melatonin. Journal of hypertension. 2014; 32(6):1264–1274. [PubMed: 24751595]

21. Steinman RM. The dendritic cell system and its role in immunogenicity. Annual review of immunology. 1991; 9(1):271–296.

22. Astrid P, et al. Potential Role for Dendritic Cells in Endothelial Dysfunction, Diabetes and Cardiovascular Disease. Current Pharmaceutical Design. 2017; 23(10):1435–1444. [PubMed: 28120714]

23. Liu M, et al. Intestinal Dendritic Cells Are Altered in Number, Maturity and Chemotactic Ability in Fulminant Hepatic Failure. PLoS One. 2016; 11(11)

24. Hansen M, Andersen MH. The role of dendritic cells in cancer. Seminars in Immunopathology. 2016:1–10.

25. Vacas-Cordoba E, et al. Dendrimers as nonviral vectors in dendritic cell-based immunotherapies against human immunodeficiency virus: steps toward their clinical evaluation. Nanomedicine (Lond). 2014; 9(17):2683–702. [PubMed: 25529571]

26. Liao X, Reihl AM, Luo XM. Breakdown of Immune Tolerance in Systemic Lupus Erythematosus by Dendritic Cells. 2016; 2016:6269157.
27. Dieterlen MT, et al. Dendritic Cells and Their Role in Cardiovascular Diseases: A View on Human Studies. 2016; 2016:5946807.
28. Price JD, Tarbell KV. The Role of Dendritic Cell Subsets and Innate Immunity in the Pathogenesis of Type 1 Diabetes and Other Autoimmune Diseases. Front Immunol. 2015; 6:288. [PubMed: 26124756]
29. Sundara Rajan S, Longhi MP. Dendritic cells and adipose tissue. Immunology. 2016; 149(4):353–361. [PubMed: 27479803]
30. Macia L, et al. Impairment of Dendritic Cell Functionality and Steady-State Number in Obese Mice. Journal of Immunology. 2006; 177(9):5997–6006.
31. Stefanovic-Racic M, et al. Dendritic cells promote macrophage infiltration and comprise a substantial proportion of obesity-associated increases in CD11c+ cells in adipose tissue and liver. Diabetes. 2012; 61(9):2330–9. [PubMed: 22851575]
32. Kato H, et al. Adiponectin acts as an endogenous antithrombotic factor. Arteriosclerosis, thrombosis, and vascular biology. 2006; 26(1):224–230.
33. Lee S, et al. Exercise training improves endothelial function via adiponectin-dependent and independent pathways in type 2 diabetic mice. Am J Physiol Heart Circ Physiol. 2011; 301(2):H306–14. [PubMed: 21602470]
34. Küster H, et al. MCP-1 contributes to macrophage infiltration into adipose tissue, insulin resistance, and hepatic steatosis in obesity. Journal of Clinical Investigation. 2006; 116(6):1494–505. [PubMed: 16691291]
35. Herzenberg LA, et al. Interpreting flow cytometry data: a guide for the perplexed. Nature Immunology. 2006; 7(7):681–685. [PubMed: 16785881]
36. Pfaffl MW. A new mathematical model for relative quantification in real-time RT-PCR. Nucleic Acids Res. 2001; 29(9):e45. [PubMed: 11328886]
37. Wentworth JM, et al. Pro-inflammatory CD11c+CD206+ adipose tissue macrophages are associated with insulin resistance in human obesity. Diabetes. 2010; 59(7):1648–56. [PubMed: 20357360]
38. Zhang L, et al. The inflammatory changes of adipose tissue in late pregnant mice. J Mol Endocrinol. 2011; 47(2):157–65. [PubMed: 21697073]
39. Kosteli A, et al. Weight loss and lipolysis promote a dynamic immune response in murine adipose tissue. J Clin Invest. 2010; 120(10):3466–79. [PubMed: 20877011]
40. Zhang H, et al. Interferon-gamma induced adipose tissue inflammation is linked to endothelial dysfunction in type 2 diabetic mice. Basic Res Cardiol. 2011; 106(6):1135–45. [PubMed: 21826531]
41. Withers SB, et al. cGMP-dependent protein kinase (PKG) mediates the anticontractile capacity of perivascular adipose tissue. Cardiovasc Res. 2014; 101(1):130–7. [PubMed: 24095868]
42. Chistiakov DA, et al. Myeloid dendritic cells: Development, functions, and role in atherosclerotic inflammation. Immunobiology. 2015
43. Yun TJ, et al. Isolation and Characterization of Aortic Dendritic Cells and Lymphocytes in Atherosclerosis. Methods Mol Biol. 2017:6786–5_29.
44. Grant R, et al. Quantification of adipose tissue leukocytosis in obesity. Methods Mol Biol. 2013; 1040:195–209. [PubMed: 23852606]
45. Stefanovic-Racic M, et al. Dendritic cells promote macrophage infiltration and comprise a substantial proportion of obesity-associated increases in CD11c+ cells in adipose tissue and liver. Diabetes. 2012; 61(9):2330–2339. [PubMed: 22851575]
46. Probst H, et al. Histological analysis of CD11c-DTR/GFP mice after in vivo depletion of dendritic cells. Clinical & Experimental Immunology. 2005; 141(3):398–404. [PubMed: 16045728]
47. Patsouris D, et al. Ablation of CD11c-positive cells normalizes insulin sensitivity in obese insulin resistant animals. Cell Metab. 2008; 8(4):301–9. [PubMed: 18840360]

48. Even SE, et al. Crosstalk between adipose tissue and blood vessels in cardiometabolic syndrome: implication of steroid hormone receptors (MR/GR). Horm Mol Biol Clin Investig. 2014; 19(2):89–101.
49. Lastra G, Manrique C. Perivascular adipose tissue, inflammation and insulin resistance: link to vascular dysfunction and cardiovascular disease. Horm Mol Biol Clin Investig. 2015; 22(1):19–26.
50. Bobryshev YV. Dendritic cells in atherosclerosis: current status of the problem and clinical relevance. European Heart Journal. 2005; 26(17):1700–1704. [PubMed: 15855191]
51. Niessner A, et al. Pathogen-sensing plasmacytoid dendritic cells stimulate cytotoxic T-cell function in the atherosclerotic plaque through interferon-α. Circulation. 2006; 114(23):2482–2489. [PubMed: 17116765]
52. Libby P, et al. Macrophages and atherosclerotic plaque stability. Current opinion in lipidology. 1996; 7(5):330–335. [PubMed: 8937525]
53. Xu XH, et al. Toll-like receptor-4 is expressed by macrophages in murine and human lipid-rich atherosclerotic plaques and upregulated by oxidized LDL. Circulation. 2001; 104(25):3103–3108. [PubMed: 11748108]
54. Weisberg SP, et al. Obesity is associated with macrophage accumulation in adipose tissue. J Clin Invest. 2003; 112(12):1796–808. [PubMed: 14679176]
55. Boutens L, Stienstra R. Adipose tissue macrophages: going off track during obesity. Diabetologia. 2016; 59(5):879–94. [PubMed: 26940592]
56. Beckman JA, Creager MA, Libby P. Diabetes and atherosclerosis: epidemiology, pathophysiology, and management. Jama. 2002; 287(19):2570–2581. [PubMed: 12020339]
57. Mangge H, et al. Low grade inflammation in juvenile obesity and type 1 diabetes associated with early signs of atherosclerosis. Experimental and clinical endocrinology & diabetes: official journal, German Society of Endocrinology [and] German Diabetes Association. 2004; 112(7):378–382.
58. McKenna HJ, et al. Mice lacking flt3 ligand have deficient hematopoiesis affecting hematopoietic progenitor cells, dendritic cells, and natural killer cells. Blood. 2000; 95(11):3489–3497. [PubMed: 10828034]
59. Hochweller K, et al. A novel CD11c. DTR transgenic mouse for depletion of dendritic cells reveals their requirement for homeostatic proliferation of natural killer cells. European journal of immunology. 2008; 38(10):2776–2783. [PubMed: 18825750]
60. Xie L, et al. Interactive Changes between Macrophages and Adipocytes. Clinical & Vaccine Immunology Cvi. 2010; 17(4):651–9. [PubMed: 20164250]
61. Doughty L, et al. The compensatory anti-inflammatory cytokine interleukin 10 response in pediatric sepsis-induced multiple organ failure. Chest. 1998; 113(6):1625–31. [PubMed: 9631803]
62. Sinuani I, et al. Role of IL-10 in the progression of kidney disease. World J Transplant. 2013; 3(4): 91–8. [PubMed: 24392313]
63. Szasz T, Bomfim GF, Webb RC. The influence of perivascular adipose tissue on vascular homeostasis. Vasc Health Risk Manag. 2013; 9:105–16. [PubMed: 23576873]
64. Ozen G, et al. Human perivascular adipose tissue dysfunction as a cause of vascular disease: Focus on vascular tone and wall remodeling. Eur J Pharmacol. 2015; 766:16–24. [PubMed: 26424111]
65. Brown NK, et al. Perivascular adipose tissue in vascular function and disease: a review of current research and animal models. Arteriosclerosis Thrombosis & Vascular Biology. 2014; 34(8):1621.
66. Ma L, et al. Perivascular fat-mediated vascular dysfunction and remodeling through the AMPK/mTOR pathway in high-fat diet-induced obese rats. Hypertension Research Official Journal of the Japanese Society of Hypertension. 2010; 33(5):446–53. [PubMed: 20186150]

Highlights

- Using a mouse model of type 2 diabetes (T2DM) dendritic cells were shown to accumulate in perivascular adipose tissue (PVAT).
- Accumulation of dendritic cells, in T2DM, was associated with increased expression of pro-inflammatory factors and decreased expression of anti-inflammatory factors.
- Accumulation of dendritic cells, in T2DM, was associated with vascular dysfunction and an inability of PVAT to enhance vasodilation.
- Genetic depletion of dendritic cells, in T2DM, improved the inflammatory environment and PVAT modulation of vascular function.

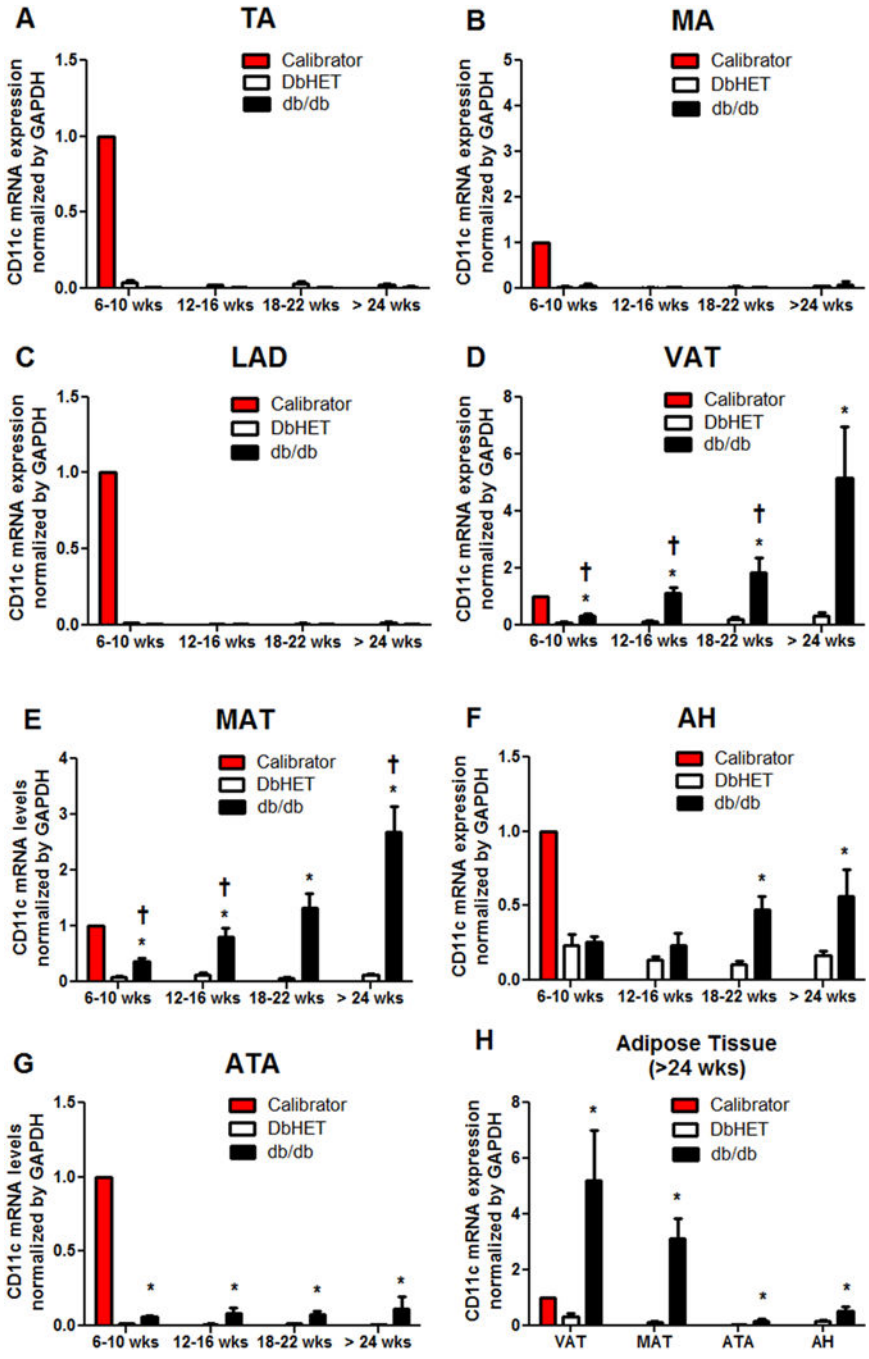

Figure 1. CD11c mRNA expression in regional and perivascular fat (PVAT)

Panels **A–C** show expression levels for thoracic aorta (TA), mesentery artery (MA) and left anterior descending coronary artery (LAD), respectively. No significant differences in CD11c mRNA expression were detected between DbHET and *db/db* mice at any age group age studied. Panels **D–G** show levels of CD11c mRNA expression in visceral adipose tissue (VAT), mesenteric adipose tissue (MAT), pericardial adipose tissue (AH) and peri-aortic adipose tissue (ATA), respectively. In general, CD11c mRNA expression was higher in adipose tissue from *db/db* mice compared to DbHET mice and increased with duration or

progression of diabetes. Panel **H** shows a summary of adipose tissue data in the greater than 24 weeks age group. Highest expression CD11c mRNA levels were observed in VAT and MAT of db/db mice. Data are shown as mean ± SEM. n=6 in per group. *: $P < 0.05$ between *db/db* and DbHET mice. †: $P < 0.05$ in *db/db* mice between >24 weeks and other age groups.

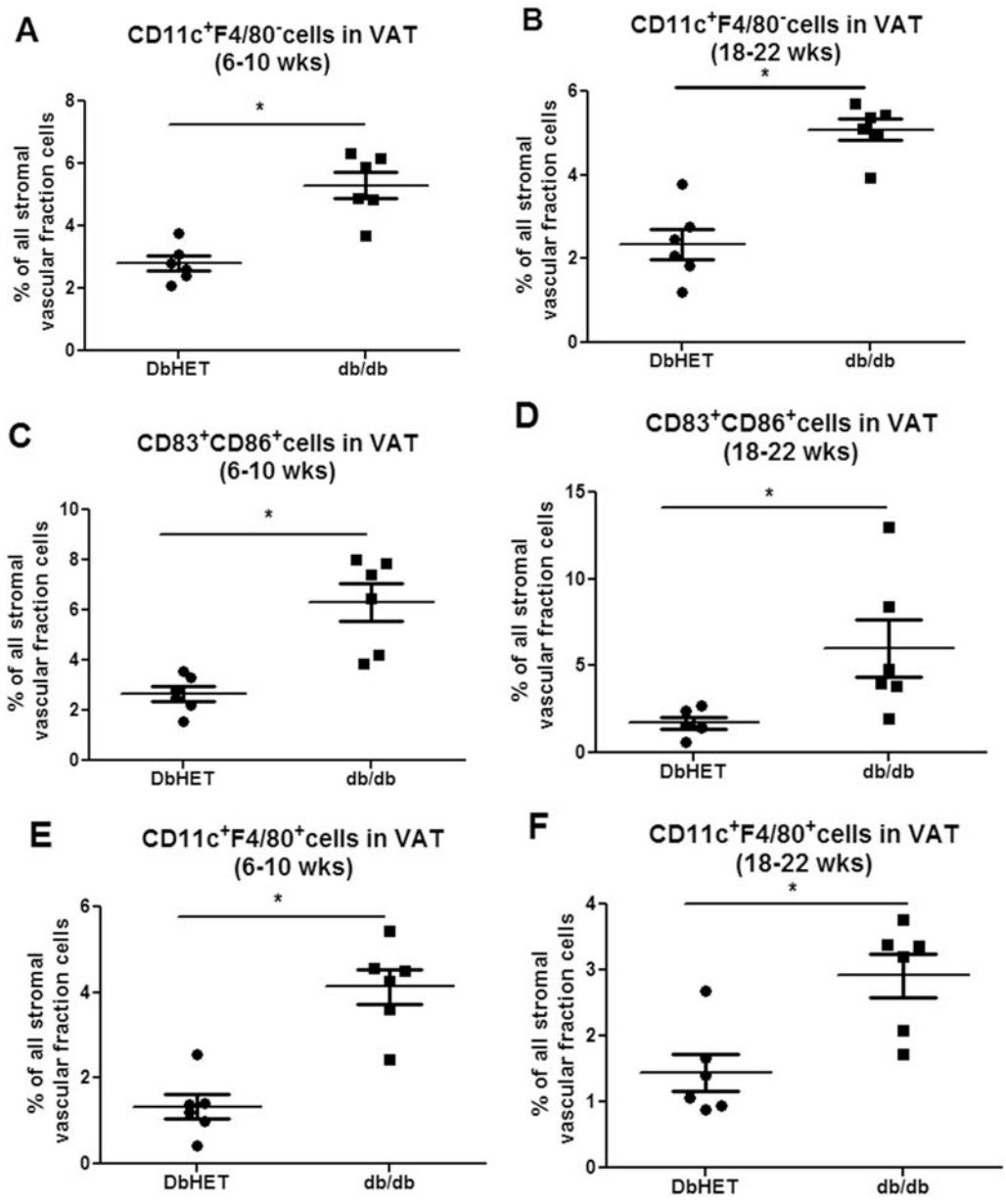

Figure 2. Increased infiltration of dendritic cells and M1 macrophages in VAT of *db/db* mice

Panel A: number of $CD11c^{+}F4/80$_dendritric cells within the stromal vascular fraction (expressed as a % of total cells). Left graph shows data for mice at 6-10 weeks of age and the right 18-22 weeks of age. **Panel B:** number of $CD11c^{+}F4/80^{+}$ M1 macrophages (%). **Panel C:** number of $CD83^{+}CD86^{+}$ dendritic cells within the stromal vascular fraction (%). Data are shown as mean ± SEM. N = 6 per group. *: $P < 0.05$ between DbHET and *db/db* mice.

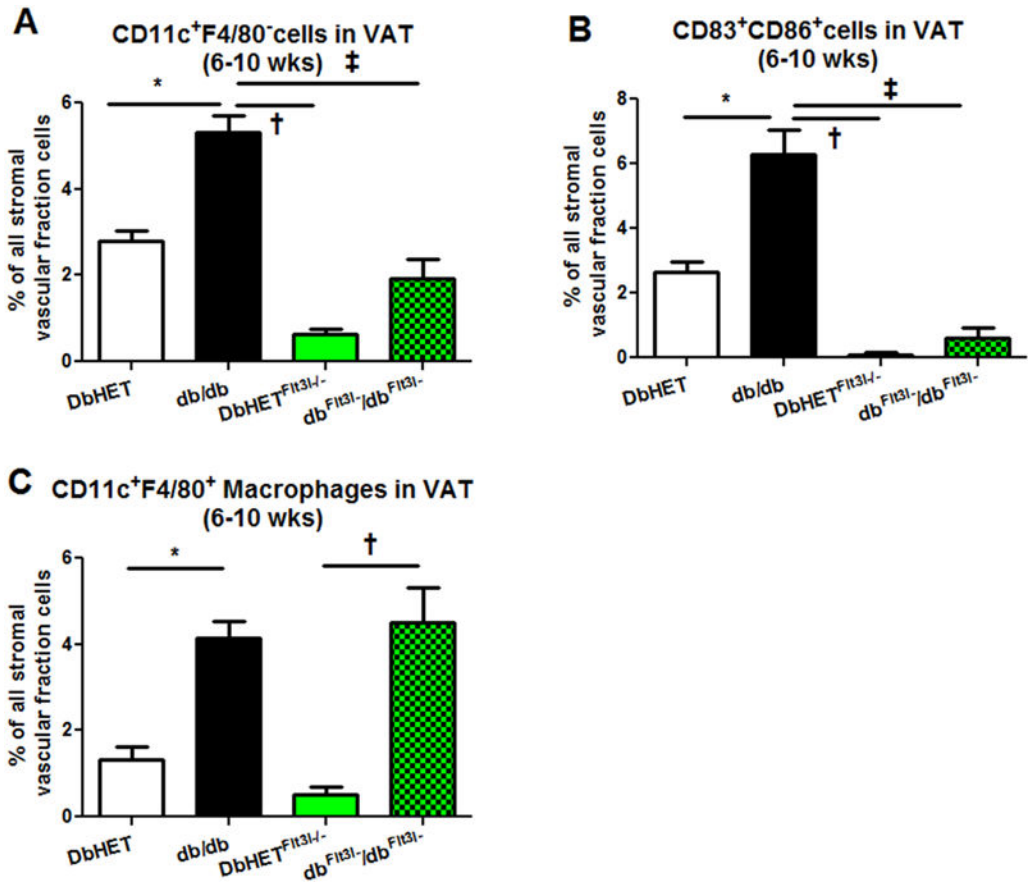

Figure 3. Summary data for dendritic cells and macrophages populations in VAT from DbHET, db/db, DbHET $^{Flt3l-/-}$ and db^{Flt3l-}/db^{Flt3l-} mice (age 6-10 weeks)

Panel A: Increased numbers of CD11c^{+}F4/80^{-} dendritic cells were detected in VAT of db/db mice compared to DbHET controls. Depletion of Flt3l gene significantly decreased CD11c^{+}F4/80^{-} dendritic cell numbers in db^{Flt3l-}/db^{Flt3l-} mice. **Panel B:** Similarly, CD83^{+}CD86^{+} dendritic cells populations were increased in db/db mice while Flt3l depletion reduced CD83^{+}CD86^{+} dendritic cells numbers in db^{Flt3l-}/db^{Flt3l-} mice. **Panel C:** An increase of CD11c^{+}F4/80^{+} macrophages was observed in VAT of db/db mice compared to DbHET controls. However, depletion of Flt3l gene did not affect macrophage numbers in db^{Flt3l-}/db^{Flt3l-} mice. Data are shown as mean ± SEM. *: $P < 0.05$. between db/db and DbHET mice. †: $P < 0.05$. between db/db and DbHET $^{Flt3l-/-}$mice, ‡: $P < 0.05$. between db/db and db^{Flt3l-}/db^{Flt3l-} mice.

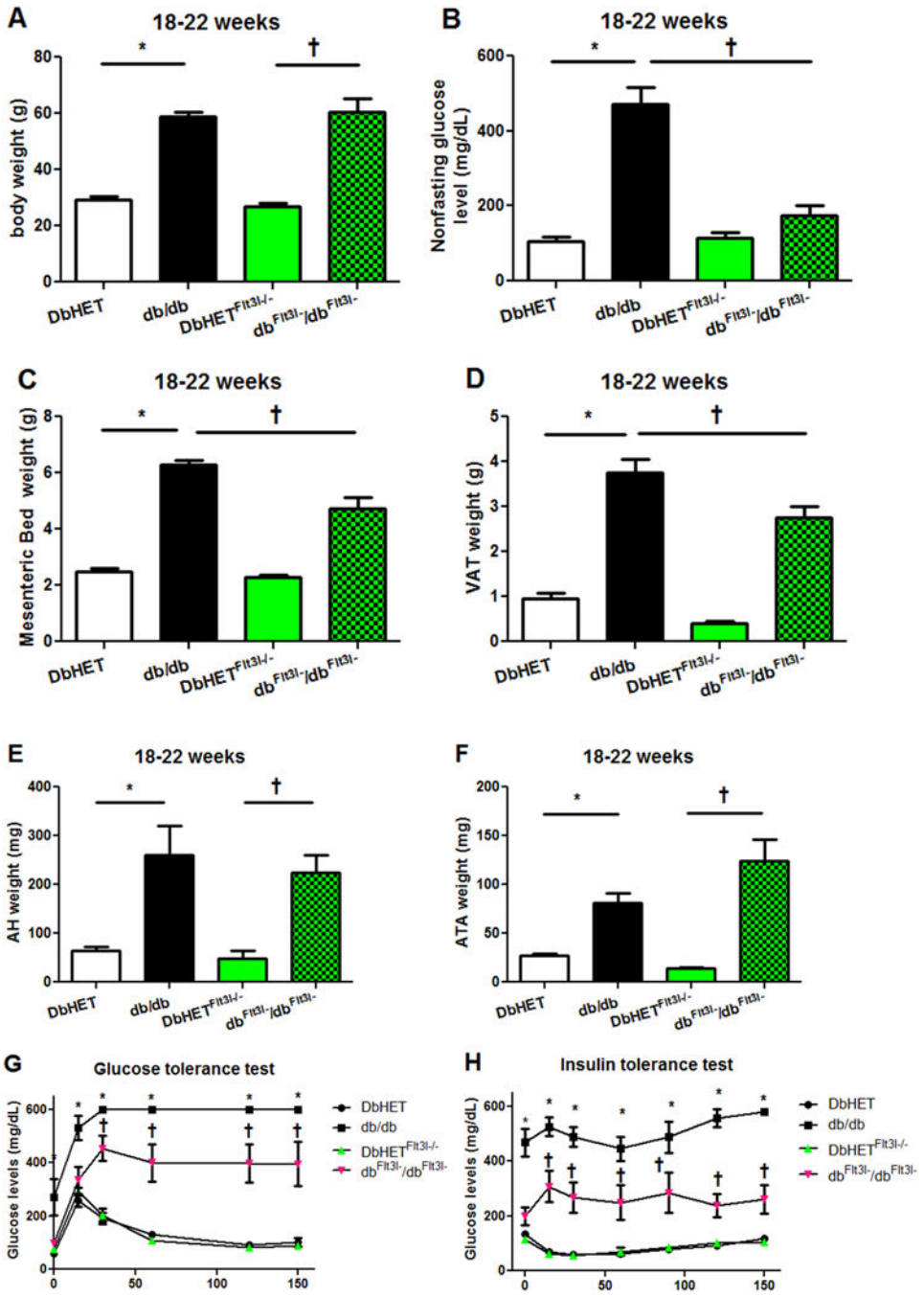

Figure 4. Effects of dendritic cell depletion on the physical characteristics of mice (age 18-22 weeks)

Panel A: db/db and db^{Flt3l-}/db^{Flt3l-} showed similar body weights while being significantly heavier than their respective control groups. Panel B: db/db mice exhibit significantly higher random blood glucose measurements than DbHET and db^{Flt3l-}/db^{Flt3l-} **Panels C – F:** db/db and db^{Flt3l-}/db^{Flt3l-} mice showed significantly higher fat depot (MAT, VAT, AH and ATA, respectively) weights. However, db^{Flt3l-}/db^{Flt3l-} showed a reduced weight of MAT and VAT compared to db/db mice**. Panels G and H** show results of glucose and insulin tolerance

tests, respectively. db/db and db^{Flt3l-}/db^{Flt3l-} mice showed significantly impaired glucose tolerance and insulin sensitivity compared to their respective control groups. Dendritic cell depletion (db^{Flt3l-}/db^{Flt3l-}) caused a partial improvement in these parameters compared to db/db mice. Data are shown as mean ± SEM. *, †: $P < 0.05$. In **G** and **H**, *: *db/db* v.s. other three groups of mice. †: *db*$^{Flt3l-}$/*db*$^{Flt3l-}$ mice v.s. DbHET or DbHET$^{Flt3l-/-}$ mice.

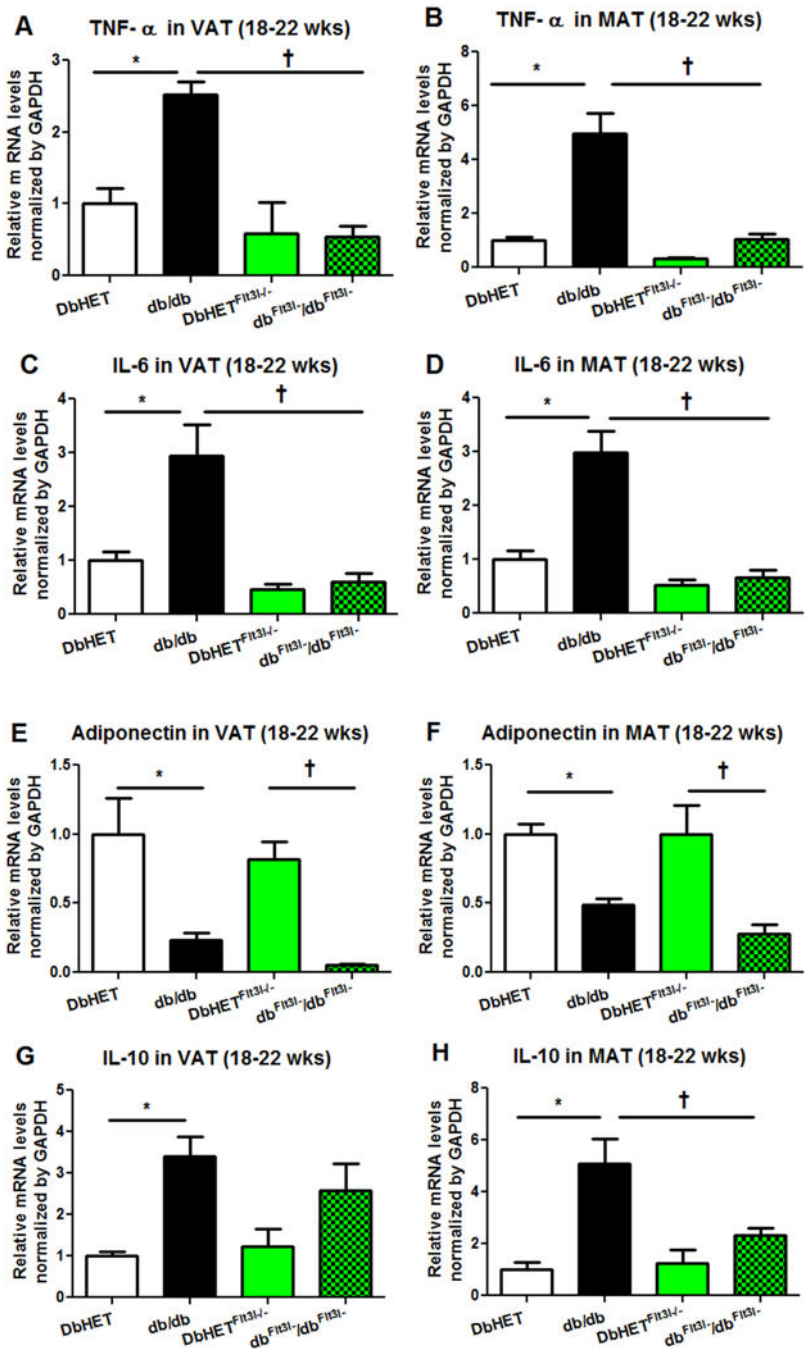

Figure 5. Tissue mRNA expression for pro-inflammatory and anti-inflammatory factors (age 18-22 weeks)

Panel A: db/db mice show higher VAT expression of mRNA for TNFα compared to DbHET mice. Dendritic cell depletion (db^{Flt3l-}/db^{Flt3l-}) normalized TNFα mRNA expression levels. **Panel B:** similar results were found for TNFα mRNA expression in MAT. **Panels C and D**: Dendritic cell depletion (db^{Flt3l-}/db^{Flt3l-}) also normalized IL-6 mRNA expression levels in VAT and MAT, respectively. **Panels E and F:** VAT and MAT expression levels of mRNA for adiponectin were lower in both db/db and db^{Flt3l-}/db^{Flt3l-} mice compared to their respective

control groups. **Panels G and H:** VAT and MAT expression levels of mRNA for IL-10 were higher in db/db mice compared to the DBHET control group. Dendritic cell depletion (db^{Flt3l-}/db^{Flt3l-}) normalized IL-10 expression levels in MAT with a trend to do so in VAT. N = 6 per group. Data are shown as mean ± SEM. *, †: $P < 0.05$.

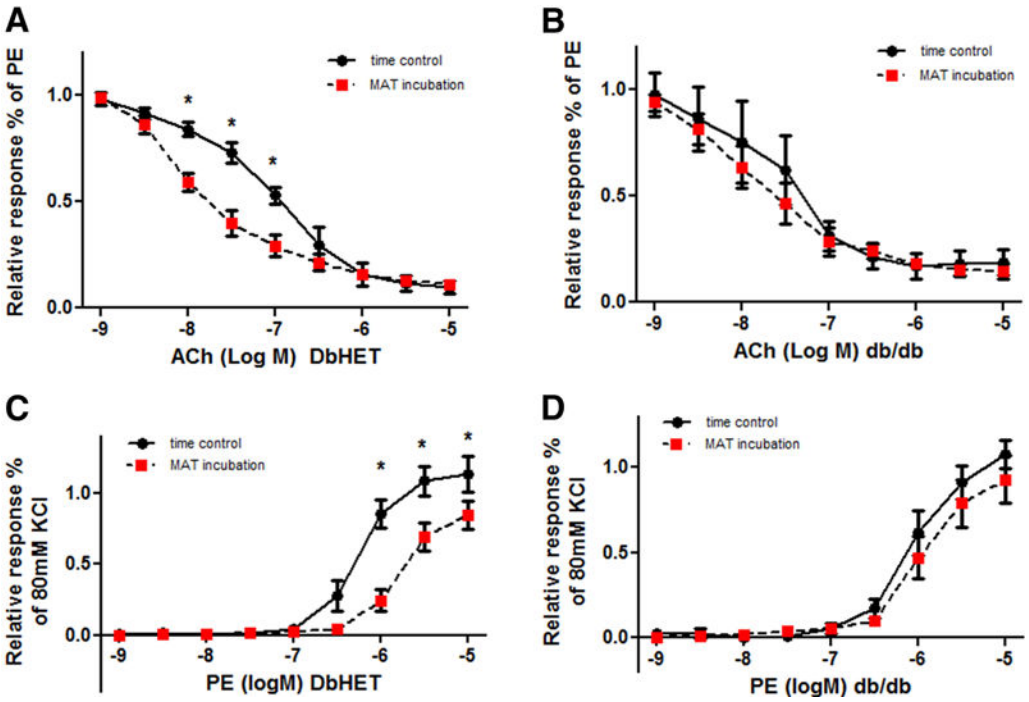

Figure 6. Effect of PVAT on vasoreactivity of DbHet and db/db mice (age 6-10 weeks)

Vasomotor responses to the vasodilator, acetylcholine (ACh) and vasoconstrictor, phenylephrine (PE), were measured in the absence (time control) and presence of MAT using wire myography (see Methods for details). Left hand column shows data for DbHET mice and the right for db/db mice. In DbHET incubation of vessel segments with PVAT caused increased sensitivity to ACh as indicated by a leftward shift in the concentration-response curve (A). In db/db mice PVAT did not increase responsiveness to ACh (B). In DbHET PVAT caused decreased sensitivity to PE as indicated by a rightward shift in the concentration-response curve (C). In db/db mice PVAT did not attenuate responsiveness to PE (D). Corresponding logEC50 values are provided in Supplementary Table 1. Data are presented as mean± SEM. N = 6 per group. *: $P < 0.05$. Concentration-response curves were analyzed by Two-way ANOVA and differences in EC50 values by Student *t*-test.

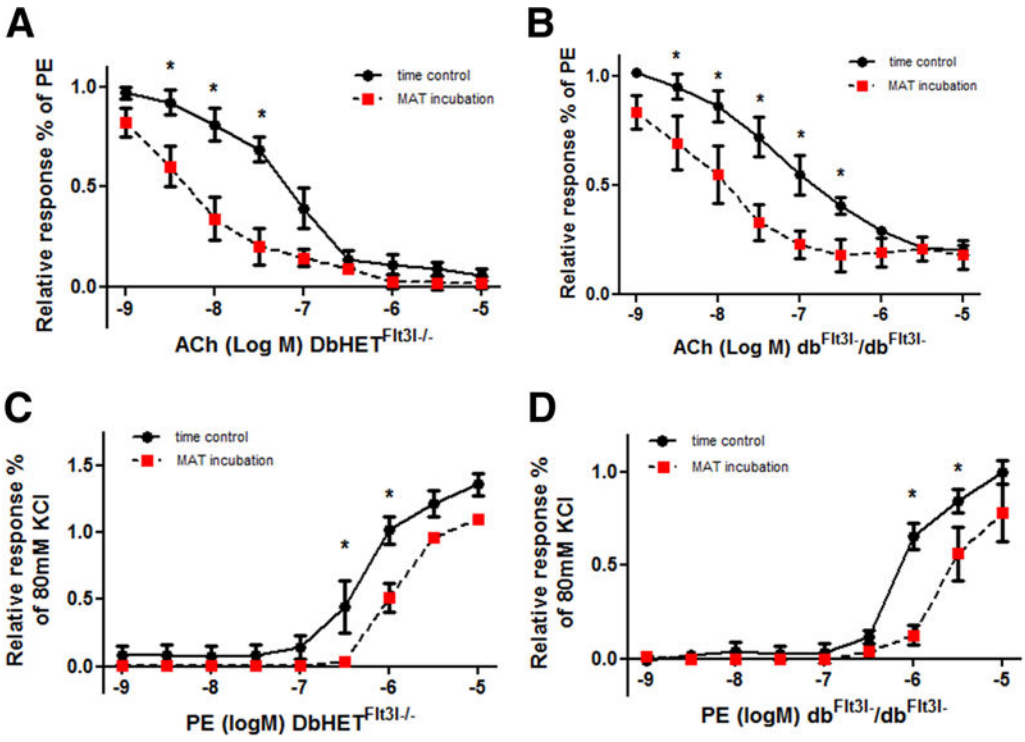

Figure 7. Effect of PVAT on vasoreactivity of DbHet $^{Flt3l-/-}$ and db/db $^{Flt3l-/-}$ mice (age 6-10 weeks)

Data were collected and analyzed as described in Figure 6. Left hand column shows data for DbHet $^{Flt3l-/-}$ mice and the right for db/db mice. In DbHET incubation of vessel segments with PVAT caused increased sensitivity to ACh as indicated by a leftward shift in the concentration-response curve (A). In db/db $^{Flt3l-/-}$ mice PVAT similarly increased responsiveness to ACh as reflected by the shift in concentration-response curves (B). In DbHet $^{Flt3l-/-}$ PVAT caused decreased sensitivity to PE as indicated by a rightward shift in the concentration-response curve (C). In db/db $^{Flt3l-/-}$ mice PVAT similarly attenuated responsiveness to PE (D). logEC50 values are provided in Supplementary Table 1. Data are presented as mean± SEM.*: $P < 0.05$. N = 6 per group.

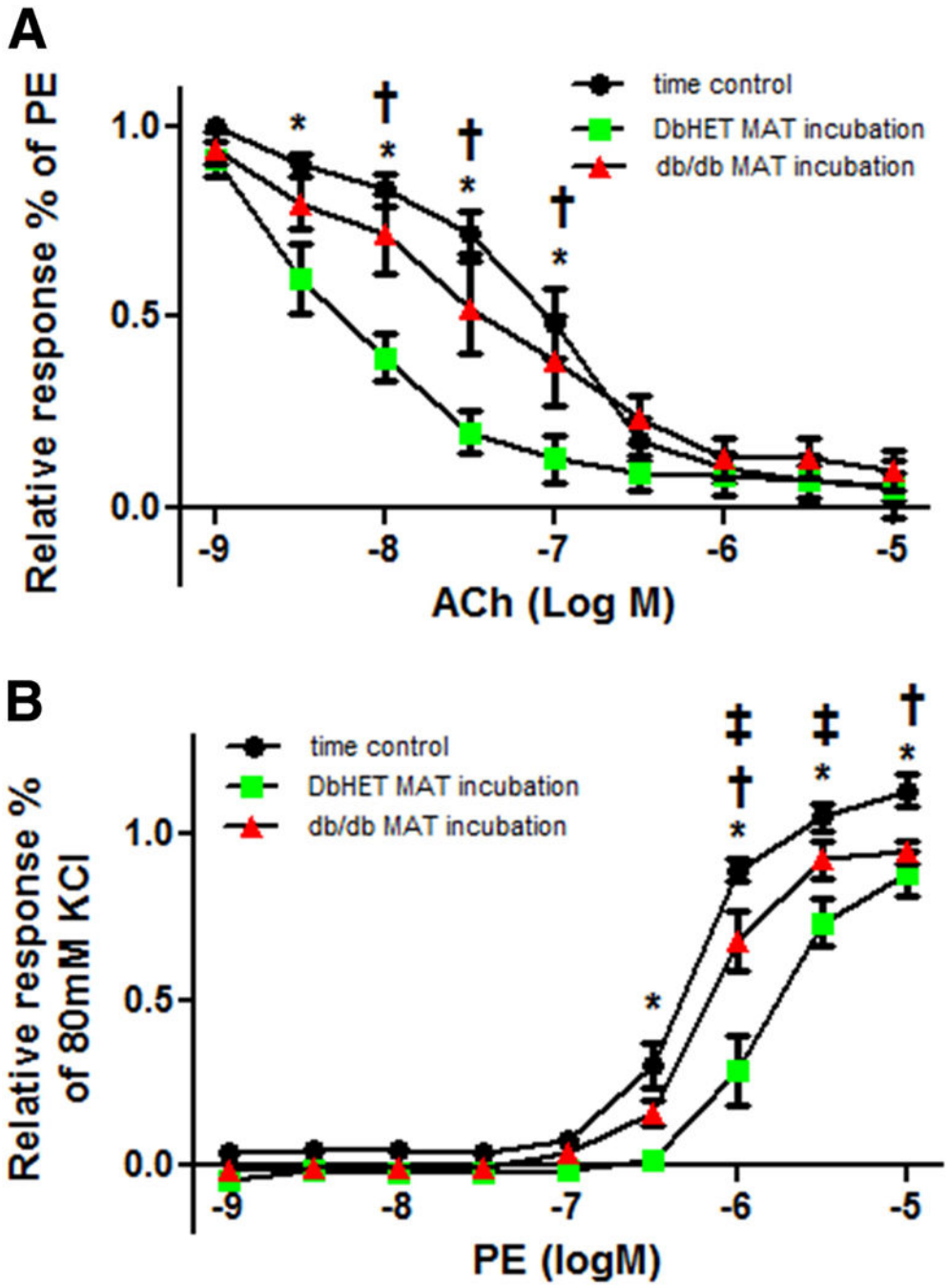

Figure 8. Acute incubation of DbHET arteries with db/db PVAT impairs vasoreactivity

Panel A: Incubation of DbHET MA with PVAT from the same animal increased sensitivity to ACh, relative to time controls (as shown in Figures 6 and 7). In contrast, the increase in sensitivity was not observed when DbHET MA was acutely (1 hour) incubated with PVAT from db/db mice. **Panel B:** Incubation of DbHET MA with PVAT from the same animal decreased sensitivity to PE, relative to time controls. In contrast, the decrease in sensitivity was not observed when DbHET MA was acutely (1 hour) incubated with PVAT from db/db mice. logEC50 values are provided in Supplementary Table 1. Data presented as mean±

SEM. N=6 per group. Concentration-response curves were analyzed by Two-way ANOVA. *: $P < 0.05$. time control vs DbHET MA+ MAT from DbHET mice. †: $P < 0.05$. time control v.s. DbHET MA+ MAT from *db/db* mice. ‡: $P < 0.05$. DbHET MA+ MAT from DbHET mice v.s. DbHET MA+ MAT from *db/db* mice.

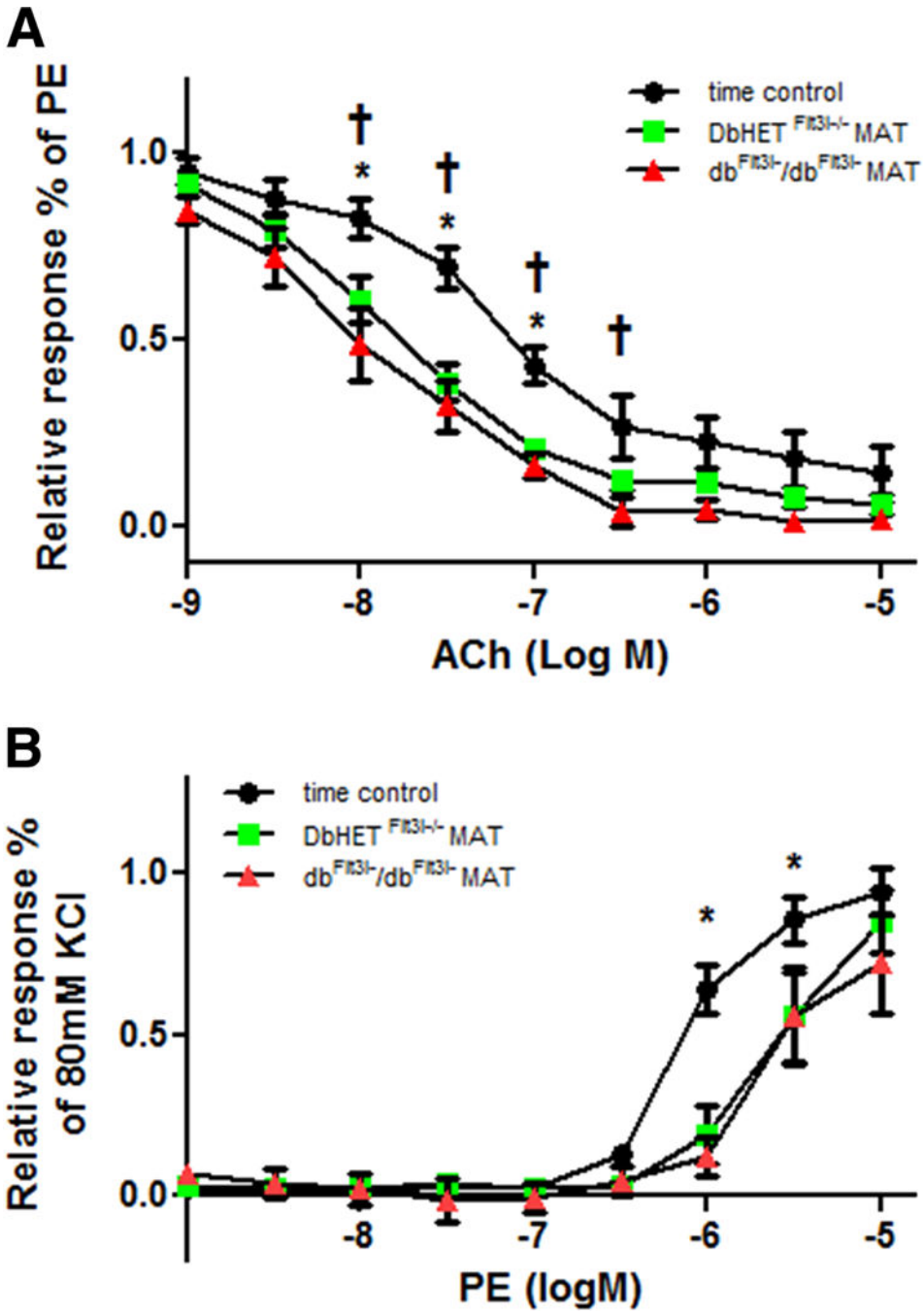

Figure 9. Acute incubation of DbHET$^{Flt3l-/-}$ arteries with *db^{Flt3l-}/db^{Flt3l-}* PVAT does not impair vasoreactivity

Data were collected and analyzed as described in previous Figures. **Panel A:** Incubation of DbHET$^{Flt3l-/-}$ MA with PVAT from the same animal increased sensitivity to ACh, relative to time controls. The increase in sensitivity was similarly seen when DbHET$^{Flt3l-/-}$ was acutely (1 hour) incubated with PVAT from *db^{Flt3l-}/db^{Flt3l-}* mice. **Panel B:** Incubation of DbHET$^{Flt3l-/-}$ MA with PVAT from the same animal decreased sensitivity to PE, relative to time controls. The decrease in sensitivity was also observed when DbHET$^{Flt3l-/-}$ MA was

acutely (1 hour) incubated with PVAT from db^{Flt3l-}/db^{Flt3l-}mice. logEC50 values are provided in Supplementary Table 1. Data are presented as mean± SEM. N=6 per group. Concentration-response curves were analyzed by Two-way ANOVA. In **(A)** *: time control v.s. DbHET$^{Flt3l-/-}$ mice. †: time control v.s. db^{Flt3l-}/db^{Flt3l-} mice. In **(B)** *: time control v.s. DbHET$^{Flt3l-/-}$ or db^{Flt3l-}/db^{Flt3l-} mice.